Indian Journal of Pure & Applied Physics
Vol. 62, April 2024, pp. 304-309
DOI: 10.56042/ijpap.v62i4.7161

A Comparative Study on Optoelectronic Properties of Dye-sensitized Solar Cells using TiO_2-ZnO Photo anodes

Kanchan Ranwa[a], Hukma Ram Khakhal[b], Preetisoni[a], Shreyas Pansambal[c], Rajender S Varma[d] & Shweta Vyas[a]*

[a]Department of Pure and Applied Chemistry, University of Kota, Kota 324 005, Rajasthan, India

[b]Department of Pure and Applied Physics, University of Kota, Kota 324 005, Rajasthan, India

[c]Department of Chemistry, Shri Saibaba College, Savitribai Phule Pune University, Shirdi 423 109, India

[d]Institute for Nanomaterials, Advanced Technologies and Innovation (CxI), Technical University of Liberec (TUL), Studentská 1402/2, 1 461 17 Liberec, Czech Republic

Received 8 December 2023; accepted 19 January 2024

In present study, dye-sensitized solar cells (DSSC) are fabricated using bare TiO_2, ZnO and TiO_2-ZnO nanocomposite via doctor's blade method with N719 sensitizer and platinum-free carbon deposited counter electrode. The ensued TiO_2-ZnO (1:1) composite films of photoanodes are characterized with UV-Vis Spectroscopy to investigate the band gaps of bare TiO_2, ZnO and their composite, in the range of 3.21- 3.31 eV. SEM studies are performed to analyze the surface morphology wherein the TiO_2-ZnO composite photoelectrode, displayed additional prominent porosities than the bare TiO_2/ZnO. The photo conversion efficiency of the cells based on TiO_2, ZnO and their composite were observed as 1.08%, 0.98%, and 1.49%, respectively, which is higher for composite due to low series resistance, high optical absorption, high recombination resistance and longer lifetime as evaluated by impedance analysis. This strategy of using TiO_2-ZnO nanocomposite photoanode could pave the way for performance improvement in a cost-effective manner for DSSCs.

Key words- Dye-sensitized solar cell; DSSC; TiO_2-ZnO composite; Impedance analysis

1 Introduction

Dye sensitized solar cells (DSSCs) initially discovered in 1991 by Gratzel and O'Regan, has garnered immense attention in presently due to the enhanced need for clean energy and its high light to current conversion efficiencies. Basically, traditional DSSC has three major components, a dye adsorbed on semiconductor layer of photoanode, an iodide/ triiodide redox system and a counter electrode with platinized layer[1]. In DSSCs, spectral sensitization of semiconductors such as TiO_2, ZnO and SnO_2 *etc*. with broad band gap is deployed to convert light into electricity[2]. To achieve a better performing device, metal complex of ruthenium-based sensitizers have been considered as highly efficient sensitizers for wide band gap semiconductors, although the costs are high. TiO_2 is one of the mostly widely deployed semiconducting oxide films due to its optical and electronic properties. It is environmentally friendly, relatively non-toxic, and stable semiconducting oxide material[3]. However, it has low carrier transmission rate due to which it cannot be used for the preparation of nanostructures with large surface area[4]. Many attempts have been made to improve TiO_2 based photoanode viz. by fusion with other semiconductor oxide (ZnO, SnO_2, Nb_2O_2 *etc*.) having broad band gap. Among these, ZnO is most preferable semiconductor material which is widely utilized for its unique electrical, optical, and photochemical properties; ZnO has almost similar band gap as TiO_2 and hence is suitable to enhance the performance of DSSCs. The composite films with varying concentrations have been developed by researchers to improve the cell performance *viz*. Giannouli investigated the effect of different ratio of TiO_2 and ZnO composite with low-cost organic dyes such as Rose Bengal and Coumarin343[5]. In addition, ZnO photoanode have also been treated with monomer dye and polymeric dye to enhance photo conversion efficiency (PCE)[6]. Recently, Kawade *et al*. in 2021 described the fabrication of (SnO_2-ZnO) composite-based device sensitized with Eosin-Y (EY) and Rose Bengal (RB) dyes. The surface morphology confirmed that the SnO_2-ZnO photo electrode has a porous nature which enhances the absorption and reported photovoltaic performance of RB sensitized

*Corresponding author: (E-mail: shwetavyas@uok.ac.in)

SnO_2-ZnO composite based device is much higher[7]. Traditionally, counter electrode of platinum have been used for long time due to its superior catalytic activity[8]. However, some reports have highlighted the formation of PtI_4 while iodide containing electrolytes are used. Thus, carbonaceous materials gained increasing attention due to their large abundance, low toxicity, minimum cost, and high catalytic activities with chemical stability against iodide containing electrolytes[9]. Herein counter electrode of carbon and photo anodes of bare TiO_2, ZnO and composite of TiO_2 and ZnO are used to study the properties of DSSC[10].

2 Materials and Method

2.1 Materials

Fluorine-doped tin oxide (FTO) (sheet resistance of 8–12 Ω/cm^2, 80% optical transmission), Degussa P25 Titanium dioxide nanopowder (99.5%, Nanoshel India), Zinc oxide nanopowder (99.5%, Nanoshel India), 4-*tert*-butylpyridine [TBP] (96% Aldrich), 1-butyl-3-methyl imidazolium iodide (BMII) (≥98% Sigma Aldrich), iodine (Sigma Aldrich) [I_2] (0.03M), acetonitrile and valero nitrile (99%, Merck), lithium iodide (LiI) (99.9%, Sigma Aldrich), N719 dye and carbon nanopowder (<100nm, 97%, Sigma Aldrich)

2.2 Experimental procedure

The procedure of fabricating DSSC is adopted from method described by Zhang *et al.*[11] with slight modification as shown in Fig. 1. TiO_2-ZnO nanocomposite paste was prepared by mixing equal amount of (0.5 g) titanium oxide (TiO_2) powder and (0.5 g) zinc oxide (ZnO) powder in 10 mL of ethanol solution. To the above mixture, 0.35 g of ethyl cellulose was added equipped with a magnetic stirrer. The composite paste was then deposited on the FTO substrate and annealed for half an hour at 450 °C. After that, the photoanodes were dipped into the solution of dye N719 for 20 hours. The electrolyte solution was prepared deploying 0.1 M LiI, 0.05 M I_2, 0.6 M BMII, and 0.5 M 4-tert-butyl pyridine in 17 mL of acetonitrile and 3 mL of Valero nitrile solution. To acquire a uniform solution, the mixture was stirred for 2 hrs. A carbon paste coated FTO was taken as a counter electrode and then the assembling of devices was accomplished by introducing iodide electrolyte in between both the electrodes.

2.3 Characterization

A field emission scanning electron microscope (FESEM) (MIRA 3 TESCAN) was used to examine the surface morphology of TiO_2, ZnO, and their composite. Using a UV/Vis/NIR spectrophotometer (PerkinElmer Lambda 750), the absorption spectra of pure TiO_2, ZnO, and their composite are recorded. Raman spectra were obtained using a 532 nm laser Raman spectrometer (Thermo Scientific DXRxi Raman imaging microscope). Impedance analyzer (Auto lab PGSTAT30) was deployed in complete darkness at 0.1 V DC and it was possible to determine the properties of fabricated devices by using TiO_2,

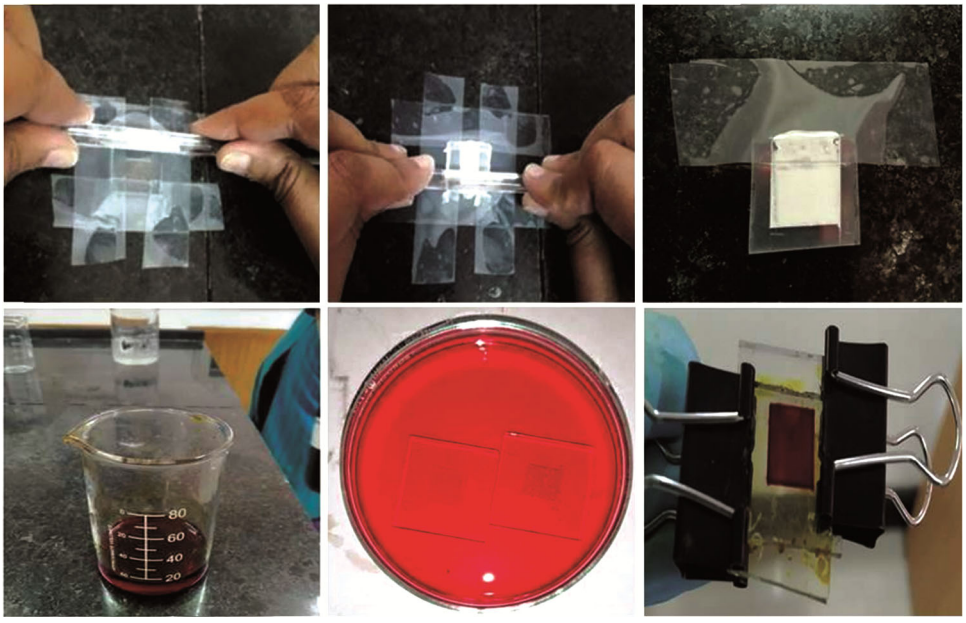

Fig. 1 — Procedure for the fabricating of DSSC.

ZnO, and their composite as a working electrode, including charge transfer, electronic processes and ionic processes. For the purpose of measuring the photovoltaic performance of DSSCs less than 1.5 AM irradiation, a solar simulator from (Verasol ORIEL LSS-7120) was deployed.

3 Results and Discussion

The absorption spectra of TiO_2, ZnO, and their composite samples were recorded in UV-visible region, (300 to 800 nm) as shown in Fig. 2(a). The absorption maxima for TiO_2, ZnO and TiO_2-ZnO composite were observed at around wavelength of 342 nm, 315 nm and 318 nm respectively. The higher absorption in the visible region was shown by TiO_2-ZnO composite sample as compared to bare TiO_2 which confirmed that the ZnO helps to improve the visible absorption of the TiO_2-ZnO composite sample and higher probability to absorb more photon for exaction dissociation than TiO_2[12-13]. On the other hand, TiO_2-ZnO composite photo-anode sample show absorption at the wavelength of 431 nm which further increased after 500 nm it may be due to better loading of N719 dye on composite, which is showing higher porosity and capability of absorbing photon in UV-Visible region in order to excite electrons from valence band to the conduction band. It demonstrated that the composite photoanode have better capacity to absorb solar light more effectively as depicted in Fig. 2(a); ZnO has good absorbance which could explain the reason for TiO_2-ZnO composite film to exhibit higher absorption than TiO_2[14].

In order to determine the bandgap of the materials, the produced TiO_2, ZnO, and TiO_2-ZnO composite-based electrodes were initially evaluated with UV-Visible NIR spectroscopy between 300 and 800 nm. The dependency of the absorption coefficient (α) on photons energy (hν) for direct permitted transition is provided by the theory of optical absorption as-

$(\alpha h\nu)^2 = (h\nu - E_g)$

The Tauc plots of different photo electrodes are shown in Fig. 2(b). The bandgap of TiO_2, ZnO, and TiO_2-ZnO composite based electrodes was determined from the Tauc Plots and found to be 3.21 eV, 3.31 eV and 3.29 eV, respectively.

3.1 Surface morphology

The surface morphology of TiO_2, ZnO and TiO_2-ZnO composite photoanode is presented in Fig 3(a) revealed the morphology of dye coated TiO_2, indicating an aggregation on the surface of FTO. An even surface of TiO_2 nanoparticles is observed in the image. The ZnO film in Fig 3(b) has high porosity and comprised a uniform layer of ZnO nanoparticles;

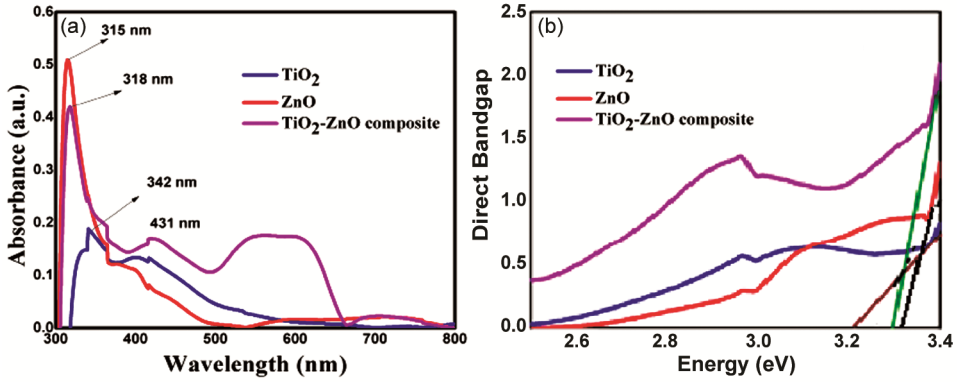

Fig. 2 — (a) Absorption spectrum of TiO_2, ZnO and composite of TiO_2 and ZnO electrode (b) Tauc plots of the photo-electrodes.

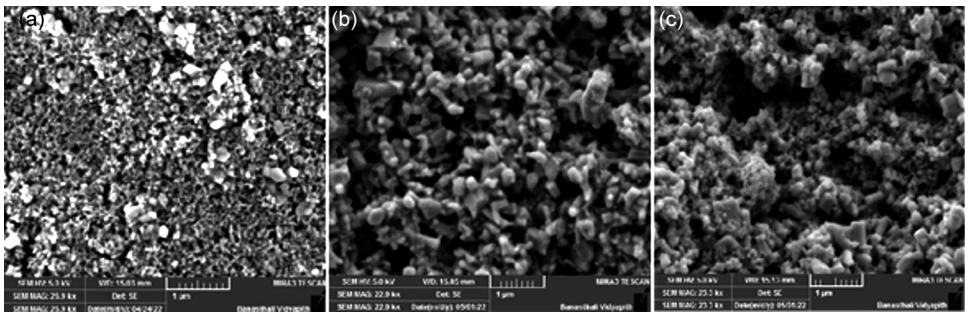

Fig. 3 — Surface morphology representation of (a) TiO_2, (b) ZnO and (c) composite TiO_2-ZnO film.

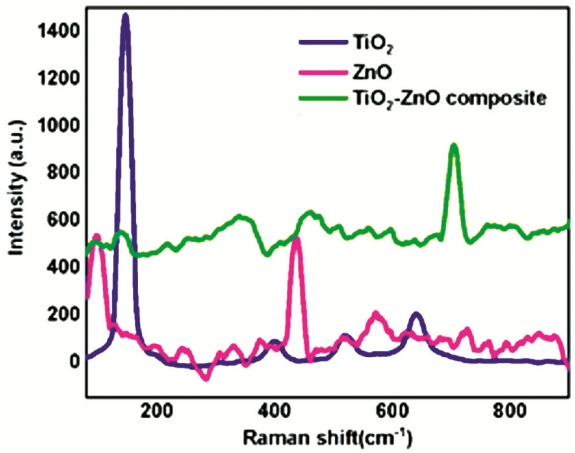

Fig. 4 — Raman spectra of TiO_2, ZnO and TiO_2-ZnO composite.

ZnO nanoparticles are more precisely visible as compared to TiO_2 presumably due to the sintering effect. The irregularities of TiO_2 film represents the aggregation of particles that could be formed during the sintering process[15]. The TiO_2 has irregular shape and evenly distributed in composite whereas ZnO exhibits cylindrical morphology of the nanoparticles. The composite represented in Fig 3(c) display cylindrical particles with uniform surface distribution with more pores as compared to bare TiO_2 and bare ZnO. This indicates that as the additional pores are produced, more the dye get attached to the composite and extra photons will be absorbed by the dye thus resulting in a better performance of composite device[16].

3.2 Raman Spectroscopy

Raman spectrum of TiO_2, ZnO and their composite film is shown in Fig 4. The typical Raman spectrum of TiO_2 displays an anatase phase with associated vibrational modes observed at 146 (E_g), 400 (B1g), 518 (A1g + B1g), and 638 (E_g) cm^{-1}, respectively[17]. The second-order Raman (E_{2H}) mode, a typical characteristic of hexagonal wurtzite ZnO, is attributed to the peak at 434 cm^{-1}. The transverse optical (TO) phonon mode is responsible for the weak peak located at around 374 cm^{-1}[18]. Surface optical (SO) phonon modes are responsible for two extra modes in the ZnO Raman spectrum, located at 517cm^{-1} and 727cm^{-1}[19]. The Raman spectrum of TiO_2-ZnO composite film shows the Raman bands belonging to TiO_2 and ZnO both and validates their presence.

3.3 Current–Voltage Characteristics

The photovoltaic performance of N719 sensitized TiO_2, ZnO and their composite based device with carbon CE is shown in Fig. 5 wherein N719 sensitized

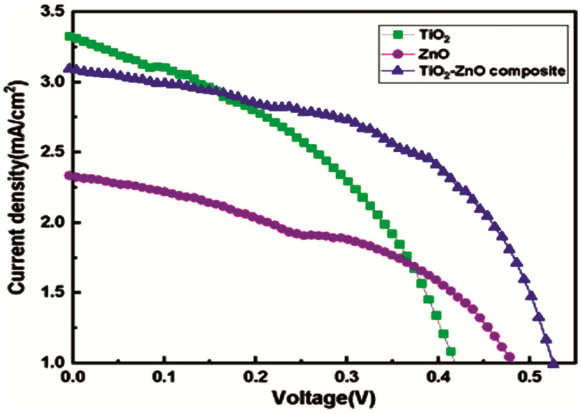

Fig. 5 — The current density–voltage characteristic (under illumination condition) of DSSCs fabricated with TiO_2, ZnO and their composite in N719 sensitizer.

Table 1 — Photovoltaic parameters of different photoanodes coated with N719 dye under Illumination condition at AM 1.5G.

Dye coated Photoanode	V_{oc}(V)	J_{sc} (mA/cm^2)	(FF)	PCE (%)
TiO_2	0.46	5.18	44.57	1.08
ZnO	0.53	3.63	51.04	0.98
TiO_2-ZnO composite	0.55	4.82	55.76	1.49

oxides are taken as a photoanode with iodide as an electrolyte and carbon-coated FTO as a counter electrode. The device performance is measured by the solar simulator under the dark in 1.5 AM condition. The photovoltaic parameters of the cell are depicted in Table 1 which reveals that the composite photoanode with carbon CE exhibits the better performance. The composite photo electrode revealed V_{oc} of 0.55 V, J_{sc} of 4.82, FF of 55.76 and overall efficiency η of 1.49 % with carbon CE which is higher than the bare TiO_2 and ZnO[20]. In TiO_2-ZnO composite photoanode, the TiO_2 nanoparticles can offer substantial surface area for the adsorption of dye molecules, while the incorporated ZnO nanoparticles which are encircled by TiO_2 nanoparticles, have ability to improve light harvesting and electron transport rate[21].

3.4 Impedance Spectroscopy

To find out more about the transport characteristics at various interfaces in the solar cell device assembly, impedance tests were carried out. The frequency range of the impedance spectra was 1 Hz to 100 kHz, and they were recorded at 0.1 V. Fig 6 shows the Nyquist plot of different photoelectrodes under the dark condition. Higher recombination resistances suggest a slower rate of electron recombination between the injected electrons and the I_3^- in the

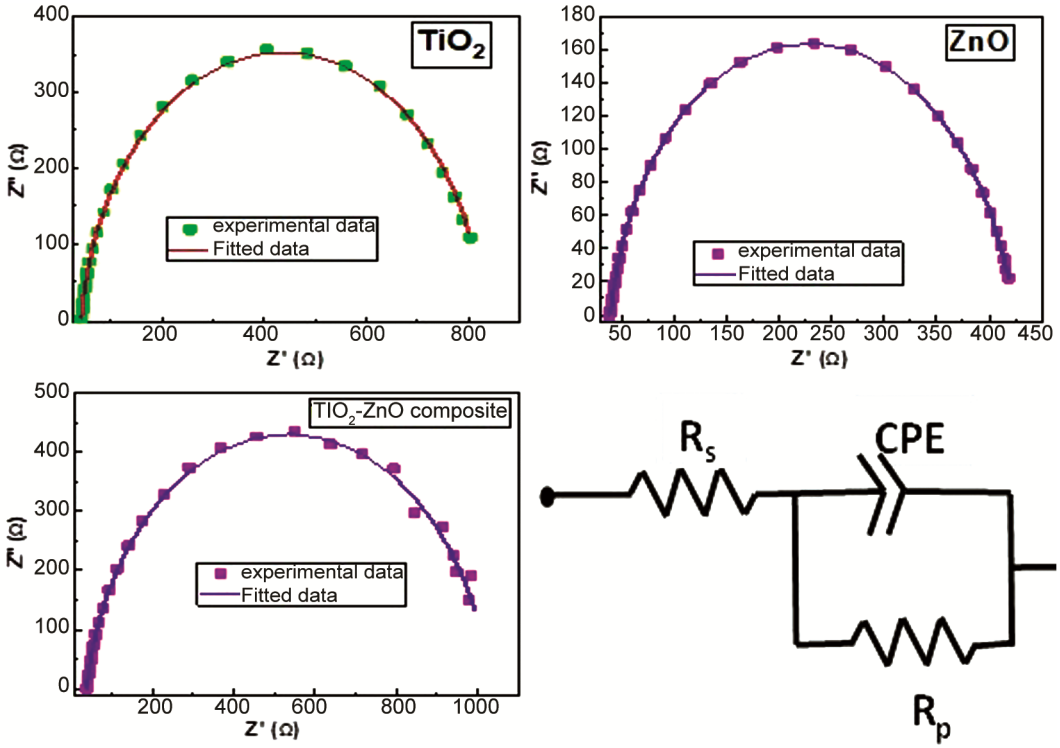

Fig. 6 — Impedance spectra TiO_2, ZnO and their composite based cell.

Table 2 — Impedance parameters of calculated by Impedance Spectroscopy.

Sr.No.	Devices with Photoanode	$R_s(\Omega)$	$R_{rec}(\Omega)$	CPE parameters		Capacitance (μF)	(C_P) τ_n(Sec)
1.	TiO_2	42.82	787.56	Q_o	n	2.68×10^{-5}	0.0212
2.	ZnO	38.87	381.32	3.52×10^{-5}	0.93	1.86×10^{-5}	0.0071
3.	TiO_2-ZnO composite	38.38	993.07	3.06×10^{-5}	0.90	1.81×10^{-5}	0.0180
				2.71×10^{-5}	0.90		

electrolyte that was constructed with composite photoanodes of TiO_2 : ZnO (1:1). The rise in short-circuit current density and conversion efficiency is consistent with these findings[22]. In photoanodes, the short-circuit current density and electron transport rate are correlated[23]. The high recombination resistance of composite electrode shows the low rate of electron hole recombination at TiO_2-ZnO composite/dye/electrolyte interface.

In bare ZnO based device, the recombination resistance decreased which is illustrated in Table 2, however, the presence of TiO_2 could be the reason for the improved results. The carrier lifetime values are precisely consistent with the recombination resistance (R_{rec}) of the devices with different photoanode[24]. Longer carrier lifetime is correlated with the higher recombination resistance. High diffusion length is also a function of long carrier lifetime, which enhances photocurrent and charge collection rates.

4 Conclusion

In this study, TiO_2-ZnO composite based photoelectrode has been prepared by a simple doctor's blade method. The N719 dye was used as a photosensitizer and carbon-coated FTO used as a counter electrode. The surface morphology of TiO_2-ZnO composite photoanode was analyzed and it was found that the composite photoanode has much porous character. The photovoltaic characteristics of TiO_2-ZnO composite based DSSCs with carbon coated CE was performed under dark condition. It has been observed that the conversion efficiency of the composite electrode based DSSC is significantly better than independent oxides. Based on our findings, it can be concluded that the TiO_2-ZnO composite based cell can be considered as the performance improving device in DSSCs.

Conflict of Interest

The authors declare no conflict of interest.

Data Availability Statement

The data that support the findings of this study are available from the corresponding author upon reasonable request.

References

1 Ocakoglu K, Harputlu E, Guloglu P & Erten-Ela S, *Synth Metal*, 162 (2012) 2125.

2 Nahida J H, Lateef K H & Fraih M R, *Iraq J Phys*, 16 (2018) 66.

3 Hosseinnezhad M & Rouhani S, *Opto-Electron Rev*, 24 (2016) 34.

4 Chang Q, Xu J, Han Y, Ehrmann A, He T & Zheng R, *J Nanomater*, (2022) 1.

5 Giannouli M, *Int J Photoenergy*, (2013) 1.

6 Singh S, Raj T, Bahadur I, Singh H & Varma R S, *Chem Select*, 7 (2022) e2022.

7 Kawade A N, Bhujbal P K, Supekar A T, Sonawane K M, Pathan H M, Shaikh S F & Al-Kaitani A A, *ES Energy Environ*, 14 (2021) 73.

8 Zhang S, Jin J, Li D, Fu Z, Gao S, Cheng S & Xiong Y, *RSC Adv*, 9 (2019) 22092.

9 Datta S, Dey A, Singha N R & Roy S, *Mater Renew Sustain Energy*, 9 (2020) 1.

10 Septiawan T Y, Sumardiasih S, Obina W M, Supriyanto A, Khairuddin & Cari C, *AIP Conf Proc* 1868 (2017) 1.

11 Zhang S, Jin J, Li D, Fu Z, Gao S, Cheng S & Xiong Y, *RSC Adv*, 9 (2019) 22092.

12 Tian J, Zhang Q, Uchaker E, Gao R, Qu X, Zhang S & Cao G, *Energy Environ Sci*, 6 (2013) 3542.

13 Samsuri S A M, Rahman M Y A & Umar A A, *Ionics*, 23 (2017) 1897.

14 Mane R S, Lee W J, Pathan H M & Han S H, *The J Phys Chem B*, 109 (2005) 24254.

15 Liao J Y, He J W, Xu H, Kuang D B & Su C Y, *J Mater Chem*, 22 (2012) 7910.

16 Liu J, Wei A, Zhao Y, Lin K & Luo F, *J Mater Sci: Mater Electron*, 25 (2014) 1122.

17 Lee K E, Gomez M A, Elouatik S, G Shan B & Demopoulos G P, *J The Electrochem Soc*, 158 (2011) H708.

18 Pandey P, Parra M R, Haque F Z & Kurchania R, *J Mater Sci: Mater Electron*, 28 (2017) 1537.

19 Alshahrie A, Alghamdi A A, Hasan P M, Ahmed F, Albalawi H M E, Umar A & Alsulami A, *Inorganics*, 10 (2022) 204.

20 Motelica L, Popescu A, Răzvan A G, Oprea O, Truşcă R D, Vasile B S & Holban A M, *Materials*, 13 (2020) 5452.

21 Kharkwal D, Sharma N, Gupta S K & Negi C M S, *AIP Conf Proc*, 2369 (2021) 020054.

22 Kharkwal D, Sharma N, S Gupta K, Mohan C & Negi S, *Sol Energy*, 230 (2021) 1133.

23 Ranjitha S, Lavanyadhevi R, Hariharan V & Anbarasan P M, *Int J Adv Sci Eng*, 5 (2018) 948.

24 Samsuri S A M, Rahman M Y A, Umar A A & Salleh M M, *Ionics*, 23 (2017) 3533.